Accuracy of the Finite Element Method with Second Order Absorbing Boundary Conditions for the Solution of Aperture Radiation Problems

John Silvestro, Xingchao Yuan[1] and Zoltan Cendes
Ansoft Corporation
Four Station Square, Suite 660
Pittsburgh, PA 15219

Abstract

The Finite Element Method with second order Absorbing Boundary Condition is a recently developed computational technique that finds use in antenna design and Electromagnetic Compatibility simulation. To determine the accuracy of this new procedure, the problem of aperture radiation was studied. The near zone and aperture fields of a waveguide antenna computed using the Finite Element Method are compared with published data and results found using other simulation techniques. These comparisons show that the new method is accurate even when the ABC boundary conforms to the problem geometry and is placed as near as $\lambda/2\pi$ to the aperture.

Introduction

A central problem in antenna design and Electromagnetic Compatibility (EMC) is computing the radiation from apertures. Apertures represent the key element in many radiating structures including open ended waveguides, flared horns and reflector antennas. In EMC, openings in system cabinets provide a major source of unwanted radiation. This latter application has become increasingly important as the European Economic Community and the FCC tighten their EMC compliance regulations.

Aperture problems have been studied in the past [1 and 2]. Typically the Method of Moments (MOM) is used to solve for the fields in the aperture assuming that the aperture is cut in an infinite ground plane. While this provides an efficient method of solution, the infinite ground plane assumption limits its utility. The resulting model is appropriate for analyzing an array of aperture antennas, but not for computing the radiation from finite sized enclosures. Real world systems are finite in size and often have irregular openings and other objects, both metal and dielectric, that affect the radiation. For such problems a hybrid approach can be used [3 and 4]. Unfortunately these methods are only appropriate for the specific geometries considered. To solve more general problems, a general purpose computer simulation tool is needed.

A technique that can easily handle complex geometries and provides a general purpose simulation procedure is the Finite Element Method (FEM). The FEM has been used successfully in the past to model closed region problems. In the FEM, the solution space is broken into small elements and the field in each element is calculated directly. The resulting discretization is usually referred to as the finite element mesh. For open region radiation problems, the solution space must be bounded. One way to accomplish this is to place a 377 Ω impedance boundary far from the radiating source. However, this approach generates a very large solution region and requires correspondingly large solution times. Recently a new Absorbing Boundary Condition (ABC) has been developed [5 and 10] that can be used to terminate the FEM mesh at boundaries very close to the radiating structure. The smaller solution region with this new absorbing boundary makes the resulting computation more efficient. However, the following question arises: How close can the new ABC be placed to the radiating structure without significant loss of accuracy? To answer this question, a study was undertaken to compare the results from FEM simulations with measured data available from the literature and with data found by using other solution techniques.

While the radiation from an opening in a system cabinet is an important problem, the

[1] Xingchao Yuan is currently employed at Cadence Design Systems, Inc., Chelmsford, MA 01824.

available data is limited. Therefore, the radiation from a waveguide antenna was chosen as the test case for this study. Using a waveguide antenna, it will be shown that this new ABC can be made to conform to the problem geometry and can be placed as close as $\lambda/2\pi$ from the aperture for such geometries. Placing the ABC this close to the radiating source keeps the FEM mesh small and results in an efficient solution.

Accuracy Statement

For the case presented here where the ABC is at $\lambda/2\pi$ the magnitude of the near zone electric field along the aperture center line is accurate to within $\pm$ 0.5 dB when compared to measured data. Also the calculation of the amplitude of the dominant mode in the aperture of an X band waveguide for the same ABC spacing is accurate to within 2 % in magnitude and 2° in phase when compared to a method of moments calculation. These numbers were found to be typical for the aperture radiation problems considered here. The apertures considered here have a maximum dimension that is on the order of 1 λ. As an example of the resources required for a solution: for the simulation of the unflanged waveguide with the ABC at $\lambda/2\pi$ (data presented in Figure 3) the run time for 3 solution passes was less than one hour on an HP 735 workstation with a 99 MHz. processor and 400 MB memory.

Overview of the FEM

To understand the results presented here it is useful to first review the basics of the FEM. See Reference 7 for more complete details on the FEM. In the FEM, the solution space is broken into small regions called finite elements. The elements used in electromagnetics are often tetrahedral as illustrated in Figure 1. This element has the advantage of being both flexible for modeling shapes and allowing closed form integrations. Since the solution space is split into small elements it is very easy to model geometries that contain different materials. This is most helpful when simulating printed circuit geometries.

The electric field in each element is approximated by using the tangential components along each edge as shown in Figure 1. This choice of approximation functions eliminates the spurious modes that can cause problems in finite element simulations [8]. The tangential electric fields are approximated by polynomials that contain unknown weighting coefficients, E_i. The electric field must satisfy the vector wave equation:

$$\nabla x \nabla x \vec{E} = k^2 \vec{E} \qquad (1)$$

The vector wave equation leads to the following variational principle:

$$F(\vec{E}) = \int (\nabla x \vec{E})^2 \, ds - k^2 \int (\vec{E})^2 \, ds \qquad (2)$$

The polynomial approximation functions are substituted into (2) and the resulting set of equations are minimized with respect to the unknown coefficients by setting the $\partial F/\partial E_i$ equal to 0 for all i. While the resulting matrix is generally large, it is sparse. This matrix equation is solved to find the unknowns, E_i.

In FEM simulation, the size, shape and location of the elements in the mesh is important to the accuracy of the solution. To reduce the possibility of a poor mesh causing inaccuracies, Delaunay tessellation and adaptive mesh refinement [16] was employed. In adaptive mesh refinement, the solution is first computed with a coarse initial mesh. The approximate solution is then substituted into the vector wave equation (1) to determine the error in each element. Next the elements that contain the largest errors are refined. The result is that the elements in those parts of the problem where the errors are the largest are reduced in size. The entire procedure is repeated until the desired accuracy is attained. In the CAE tool used here the user controls the definition of the initial mesh. The user can specify a seed value for various surfaces in the model. This seed value is the spacing of additional points added to the original problem description on a specified surface. These seed points become the vertices of the tetrahedral finite elements.

The Second Order ABC

Absorbing boundary conditions (ABCs) are of two general types. The first is the one derived by Bayliss and Turkel [9] in scalar form and then by Peterson [5] and by Webb and Kanellopoulos [10] in vector form. The basis of the derivation of this ABC is the far field expansion or Wilcox expansion [11]. The first term in this expansion provides a 377 Ω impedance boundary that must be placed relatively far from radiating sources. The second type of ABC was derived by Engquist and Majda [12] in scalar form and by Sun and Balanis [13] in vector form. This ABC is derived by splitting the operator into two first-order operators and then approximating these first-order operators. This allows waves to travel in one direction only; hence, they are often called a one-way ABCs.

In this paper the second-order ABC presented in References [5 and 10] is used. It should be noted that although these ABCs are derived in the reference, these papers are purely theoretical and do not provide numerical examples of its accuracy. The purpose of this paper is to provide such examples.

This ABC is computationally efficient for the following reasons. First, it includes higher order terms compared to the first order ABC. Second, the ABC may be applied on a conformal boundary because it absorbs the outgoing wave on a piecewise basis. Finally, the finite element shape functions themselves are second order so that the ABC boundary may be placed very close to the source of the radiation.

The above discussion indicates that the new ABC behaves very much like the absorber used in an anechoic chamber. Therefore, one would expect that the second order ABC can be placed very close to the radiating structure and can be made to conform to the geometry. From antenna theory it can be shown that the near zone of an antenna can be broken into two separate regions: the reactive near zone and the radiating near zone regions [14]. The reactive near zone is the region closest to the geometry where the reactive fields are present. It is the fields in this region that contribute to the imaginary component of the input impedance. Since these are reactive fields one does not want to place an absorber in this region else the amount of energy stored is affected. On the other hand, this should not be a concern in the radiating near zone. Therefore, one should be able to place the ABC in the radiating near zone of the geometry. Reference [14] states that the boundary between the reactive and radiating near zones may be as small as $\lambda/2\pi$ from the antenna. One would expect then that the lower limit on the ABC placement would be on the order of $\lambda/2\pi$.

Results for an Unflanged Waveguide

The computed data presented here was solved using an initial mesh that was seeded with mesh points every $\lambda/10$ over the aperture opening, over the input port and on the ABC boundary. Adaptive mesh refinement was applied twice to these initial values to perform a total of three solution passes. This was sufficient to ensure that the change in the value of the reflection coefficient from pass 2 to pass 3 was less than 0.02.

A problem with much of the waveguide antenna simulations presented in the literature is that the aperture plane is assumed to be an infinite ground plane corresponding to a waveguide with an infinite flange. While this assumption reduces the complexity of the mathematical model, it does not reflect the situation in the real world. To determine the optimum distance for placement of the ABC, it is important to simulate a geometry that does not have an infinite flange. The authors of Reference 15 considered such a problem: they studied the radiation from an unflanged WR3200 rectangular waveguide. This is the type of antenna used in large anechoic chambers for susceptibility testing. For the case considered in Reference 15 the antenna has a net input power of 44.8 watts at a frequency of 275 MHz. The FEM simulation model that was used is shown in Figure 2. This is a simple unflanged waveguide with an input port at one end. The waveguide is enclosed in a rectangular box on which is placed the ABC. The spacing D was varied and the data compared with the measured values. The results are shown in Figure 3. The data presented is the magnitude of the electric field along the x=y=0 line for a variety of values of z in the antenna's near zone. At the frequency

of operation the field points for the smaller spacings are less than 1 λ from the opening. It should be noted that these field points are outside of the FEM mesh for the cases presented here. The values of the fields determined on the boundary are used to calculate the fields at points outside of the mesh (see [6] for details). From the data shown in Figure 3, it can be seen that for D = $\lambda/4$ and $\lambda/2\pi$ the differences between measured and computed results are less than ± 0.5 dB. The $\lambda/10$ case, though, is not as accurate. These results are an additional 0.5 dB smaller than the $\lambda/2\pi$ data when compared to the measured. In fact a case could be made that at this spacing the results are still very good. The FEM meshes for the 3 spacings had approximately the same number of unknowns (within ≈10% of each other). The main difference between these three simulations was the size of the tetrahedra, not a significant increase in the number.

Another test of the solution procedure was to calculate the gain of the antenna using the far zone fields determined by the FEM/ABC approach. The gain for this antenna calculated using equation (2) in Reference 15 is 6.9 dB and the gain calculated in the simulation with D=$\lambda/2\pi$ is 6.5 dB. While the gain equation given in Reference 15 is approximate, it nevertheless indicates that a D=$\lambda/2\pi$ spacing can be used to accurately model this aperture problem. Thus, the ABC can be made to conform to the shape of the geometry and can be placed as close as $\lambda/2\pi$ from the aperture with accurate results for these geometries. Using D=$\lambda/4$ for the spacing does not significantly increase the accuracy of the results but does require a small increase in mesh size.

As a final note, the data for the $\lambda/2\pi$ and $\lambda/4$ cases appeared to converge to accurate values for the reflection coefficient after only one adaptive mesh refinement, but they were run for a second mesh refinement to be consistent with the other case.

The Aperture Fields for Flanged Waveguide Antennas

As stated in the introduction, the radiation from apertures has been studied in the past using the method of moments (MOM). Thus, the results from a MOM solution can also be used to verify the FEM simulations. Before discussing the specifics of this approach, it should be noted that this MOM procedure is designed to analyze waveguide antennas with infinite flanges only and it is not a general purpose CAE tool. In this simulation, the aperture plane is assumed to be an infinite ground plane and the aperture is closed using the equivalence principle. Equivalent magnetic currents are placed on either side of the short. These magnetic currents are approximated by a finite weighted sum of entire domain basis functions. The unknown weighting coefficients are determined using a Galerkin procedure. Vector potential modal functions were used as basis functions. The field approximation for the aperture shown in Figure 4 is as follows [2]:

$$\vec{E}_a \approx \sum_{n,m} \left[C_{nm}\, e_{y,nm}\, \hat{y} + D_{nm}\, e_{x,nm}\, \hat{x} \right] \quad (3)$$

where:

$$e_{y,nm} = \sqrt{\frac{\varepsilon_{0n}\varepsilon_{0m}}{ab}} \sin\left(\frac{n\pi x}{a}\right) \cos\left(\frac{m\pi y}{b}\right)$$
$$e_{x,nm} = \sqrt{\frac{\varepsilon_{0n}\varepsilon_{0m}}{ab}} \sin\left(\frac{m\pi y}{b}\right) \cos\left(\frac{n\pi x}{a}\right) \quad (4)$$

and where ε_{0n} is Neumann's number. Since the MOM simulation assumes an infinite flange, a small ground plane was placed around the aperture in the FEM models. The ground plane extends $\lambda/4$ from each edge of the aperture in the ±x and ±y directions. The ABC is rectangular in shape. It is located at D = $\lambda/2\pi$ from the aperture and from the edges of the ground. The apertures and the ABC were seeded in the same way as before and a total of 2 passes were run for all of the simulations in this section.

Due to the orthogonality of the basis functions of (4), it is a simple task to calculate the coefficients C_{nm} and D_{nm} from the FEM

data. To compute C_{nm} or D_{nm}, the dot product of the fields in the aperture are taken with $e_{y,nm}\hat{y}$ for C_{nm} or with $e_{x,nm}\hat{x}$ for D_{nm}, and the result is integrated numerically over the aperture. Consider the data presented in Figures 5 and 6. The magnitude and phase of the first 4 modes in an X band waveguide operated at 10 GHz are shown. It was found previously that these four modes are sufficient to accurately model the aperture field in this antenna [2]. As stated previously, the FEM and MOM data for the dominant mode are within 2% in the magnitude and 2 ° in phase.

To verify that the size of the aperture does not significantly affect the results or require a larger ABC spacing, consider the data shown in Figure 7. This is for a waveguide of twice the dimensions as an X-Band waveguide (a=1.8" and b=0.8"). It is operated at 10 GHz., making this antenna twice as large electrically as the one simulated previously. For this case the first 6 modes in the aperture are compared. The ABC was again rectangular and was spaced $\lambda/2\pi$ from the aperture and the edges of the ground. In this case there is also excellent agreement between the two sets of data, the dominant mode amplitudes are different by less than 5%.

As a final test, consider the data presented in Figure 8. For this case, there are two X band waveguide fed apertures (same dimensions as was used for Figures 5 and 6) in the ground plane. The geometry is shown in Figure 8a. The apertures are spaced 0.6" apart. One is driven and the other is connected to a matched load. Due to mutual coupling between the two aperture antennas, there is a non-zero field in the aperture of the undriven guide. The modal amplitudes of the fields in both apertures are shown in Figure 8. The ground plane again extends $\lambda/4$ beyond the apertures and the ABC spacing is $\lambda/2\pi$.

Conclusion

From the data presented here it is concluded that the new second order ABCs can be used very effectively with the finite element method to model aperture radiation problems. The new ABCs can be shaped to conform to the problem geometry and can be placed as close as $\lambda/2\pi$ from the aperture for accurate simulation. Since the finite element method is well suited to modeling real-life structures such as finite flanges and variations in enclosure shapes, it provides a new, powerful tool to analyze radiation problems efficiently.

It should be noted that these results are valid for the types of geometries presented here. It is possible that a complicated radiating geometry can be found where the reactive near zone ends at a distance that is greater than $\lambda/2\pi$. In that case, the ABC should be spaced at least that distance from the geometry for best results.

References

[1] R. F. Harrington and J. R. Mautz, "A general network formulation for aperture problems," *IEEE Trans. on Ant. and Prop.*, Vol. AP-24, pp. 870-872, Nov. 1970.

[2] J. W. Silvestro, "Mutual coupling in finite arrays of rectangular apertures," *MS Thesis*, Case Western Reserve U., 1984.

[3] X. Yuan, D. Lynch and J. Strehbehn, "Coupling of finite element and moment methods for electromagnetic scattering from inhomogeneous objects," *IEEE Trans. on Ant. and Prop.*, Vol. AP-38, pp. 386-393, Mar. 1990.

[4] J-M Jin and J. L. Volakis, "A finite element-boundary integral formulation for scattering by three dimensional cavity-backed apertures," *IEEE Trans. on Ant. and Prop.*, Vol. AP-39, pp. 97-104, Jan. 1991.

[5] A. F. Peterson, "Absorbing boundary condition for vector wave equations," *Microwave and Optical Technology Letters*, Vol. 1, pp. 62-64, Apr. 1988.

[6] *Ansoft's Maxwell SI Eminence: User's Manual*, Ansoft Corp., Pitts., PA, 1994.

[7] J. Jin, *The Finite Element Method in Electromagnetics*, John Wiley & Sons, New York, 1993.

[8] Z. J. Cendes, "Vector finite elements for electromagnetic field computation," *IEEE*

Trans. on Magnetics, Vol. MAG-27, pp. 3953-3966, 1991.

[9] A. Bayliss and E. Turkel, "Radiation boundary conditions for wave like equations," *Comm. Pure Appl. Math.,* Vol. 23, pp. 707-725, 1980.

[10] J.P. Weeb and V.N. Kanellopoulos, "Absorbing boundary conditions for the finite element solution of the vector wave equation," *Microwave and Optical Technology Letters,* Vol. 2, pp. 370-372, Apr. 1989.

[11] C.H. Wilcox, "An expansion theorem for electromagnetic fields," *Comm. Pure Appl. Math.,* Vol. 9, pp. 115-134, 1956.

[12] B. Engquist and A. Majda, "Absorbing boundary conditions for the numerical simulations of wave," *Math. Comput.,* Vol. 31, pp. 629-651, July 1977.

[13] W. Sun and C.A. Balanis, "Vector one-way absorbing boundary conditions for FEM applications'" *IEEE Trans. on Ant. and Prop.,* Vol. 42, pp. 872-878, June 1994.

[14] A.D. Yaghjian, "An overview of near field antenna measurements," *IEEE Trans. on Ant. and Prop.,* Vol. AP-34, pp. 30-45, Jan. 1986.

[15] D.I. Wu and M. Kanda, "Comparison of theoretical and experimental data for the nearfield of an open ended rectangular waveguide," IEEE *Trans. on EMC.,* Vol. AP-31, pp. 353-358, Nov. 1989.

[16] Z. J. Cendes and D. N. Shenton, "Adaptive mesh refinement in the finite element computation of magnetic fields," *IEEE Trans. on Magnetics,* Vol. MAG-21, pp. 1811-1816, Sept. 1985.

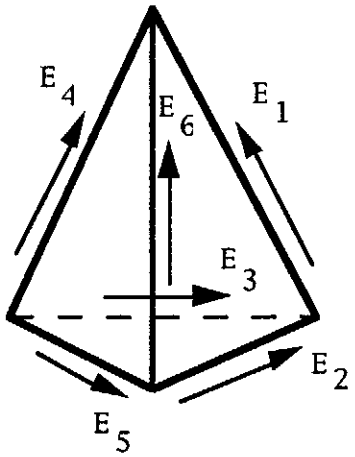

Figure 1 A tetrahedral showing the electric field components of the tangential vector finite element.

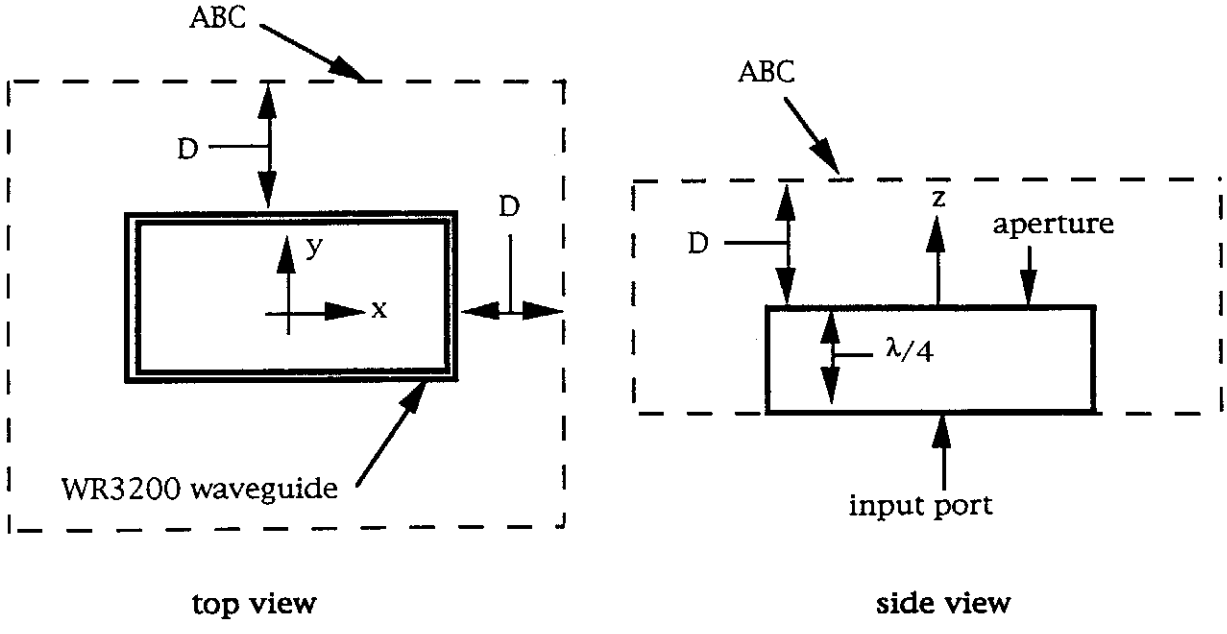

Figure 2 FEM simulation model of the unflanged rectangular waveguide antenna.

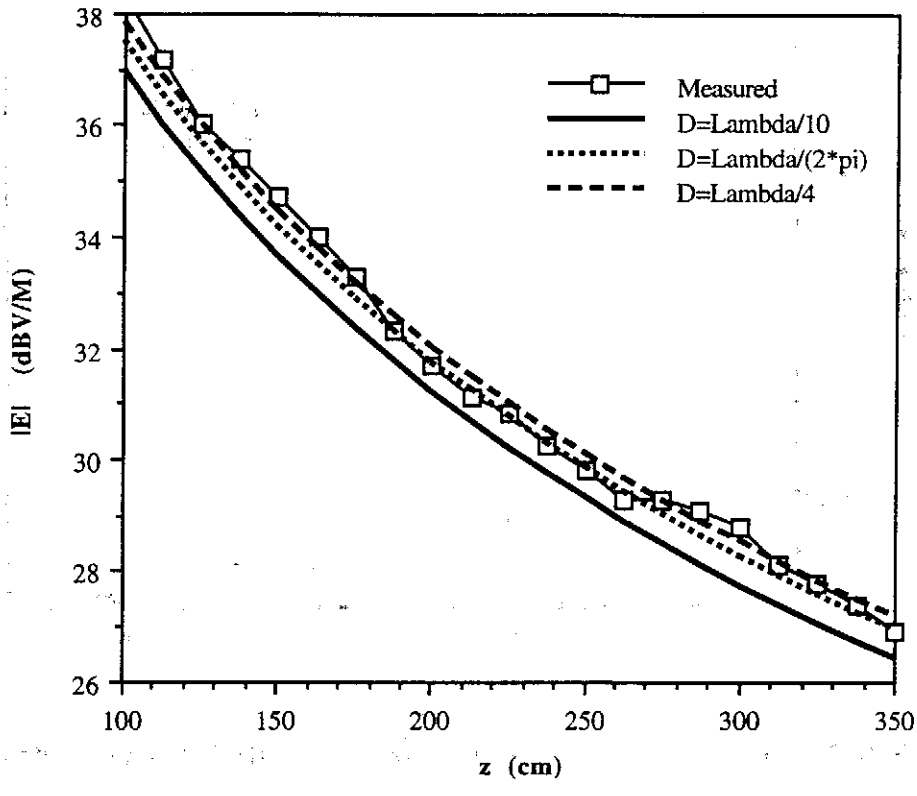

Figure 3 Magnitude of the near zone electric field along the center axis of the aperture. The values are in dBV/M.

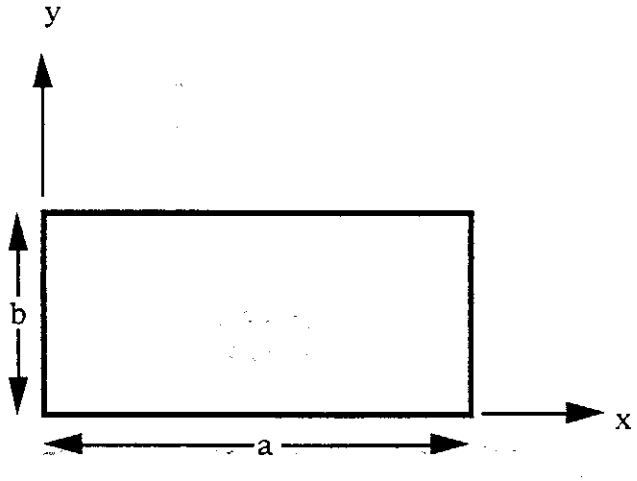

infinite ground plane (z=0)

Figure 4 The dimensions and coordinate system for the flanged waveguide antenna used in the MOM simulations. For the X band waveguide used here: a=0.9" and b=0.4".

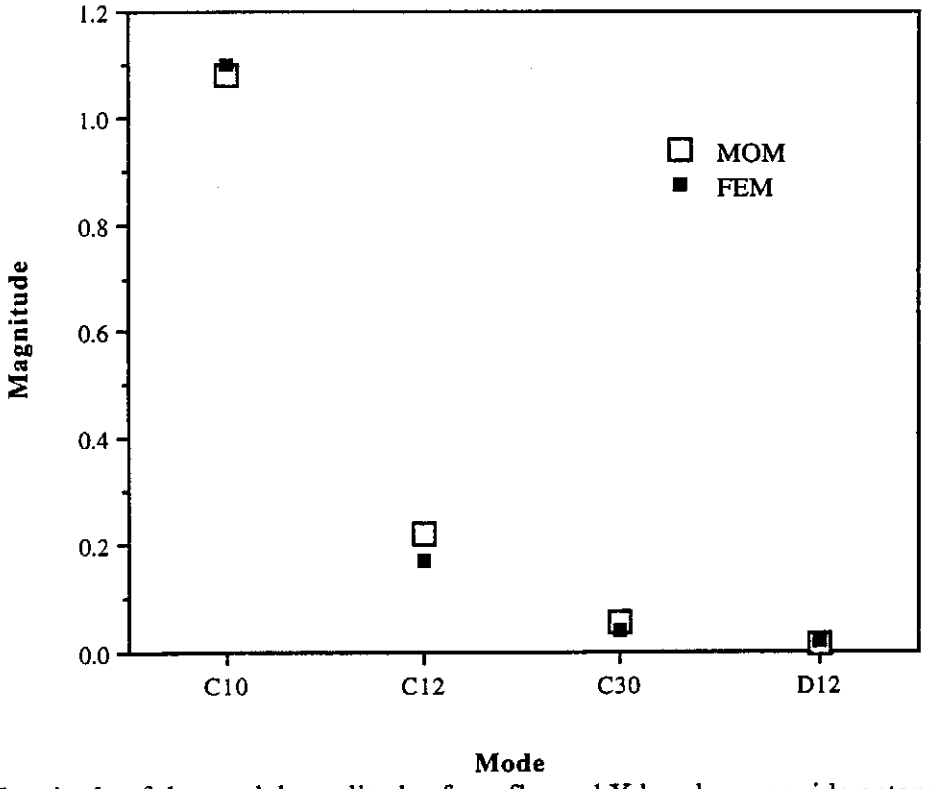

Figure 5 Magnitude of the modal amplitudes for a flanged X band waveguide antenna.

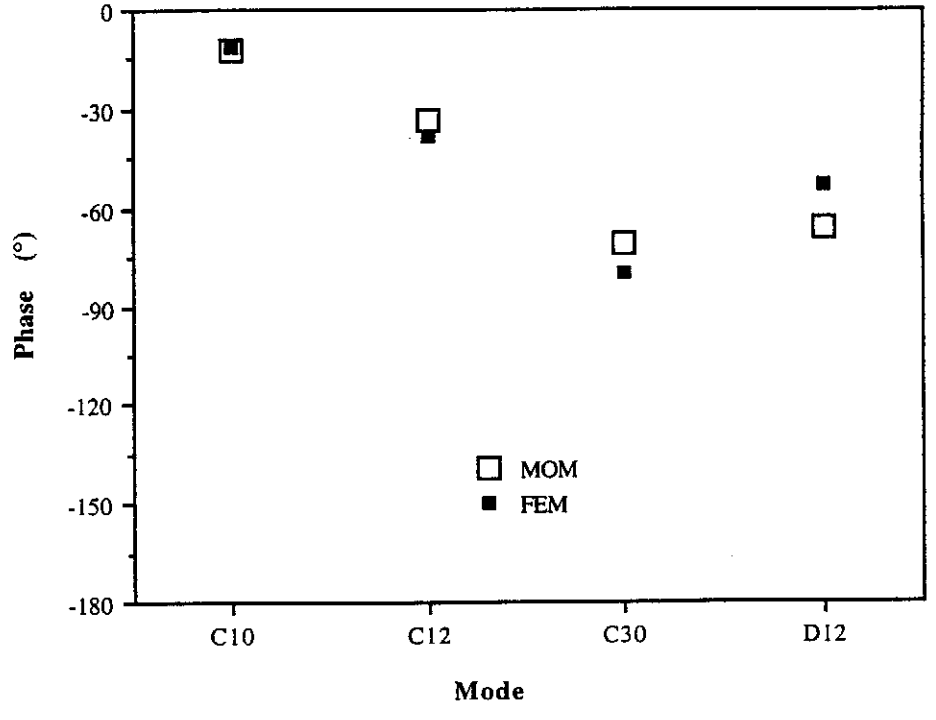

Figure 6 Phase of the modal amplitudes for a flanged X band waveguide.

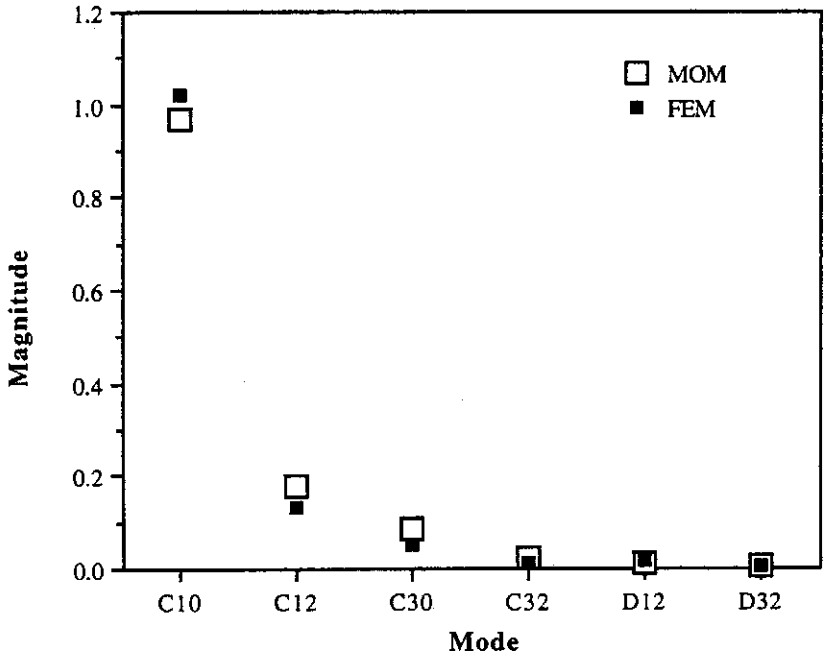

Figure 7 Magnitude of the modal amplitudes for a flanged waveguide antenna that is twice as large as a standard X band waveguide.

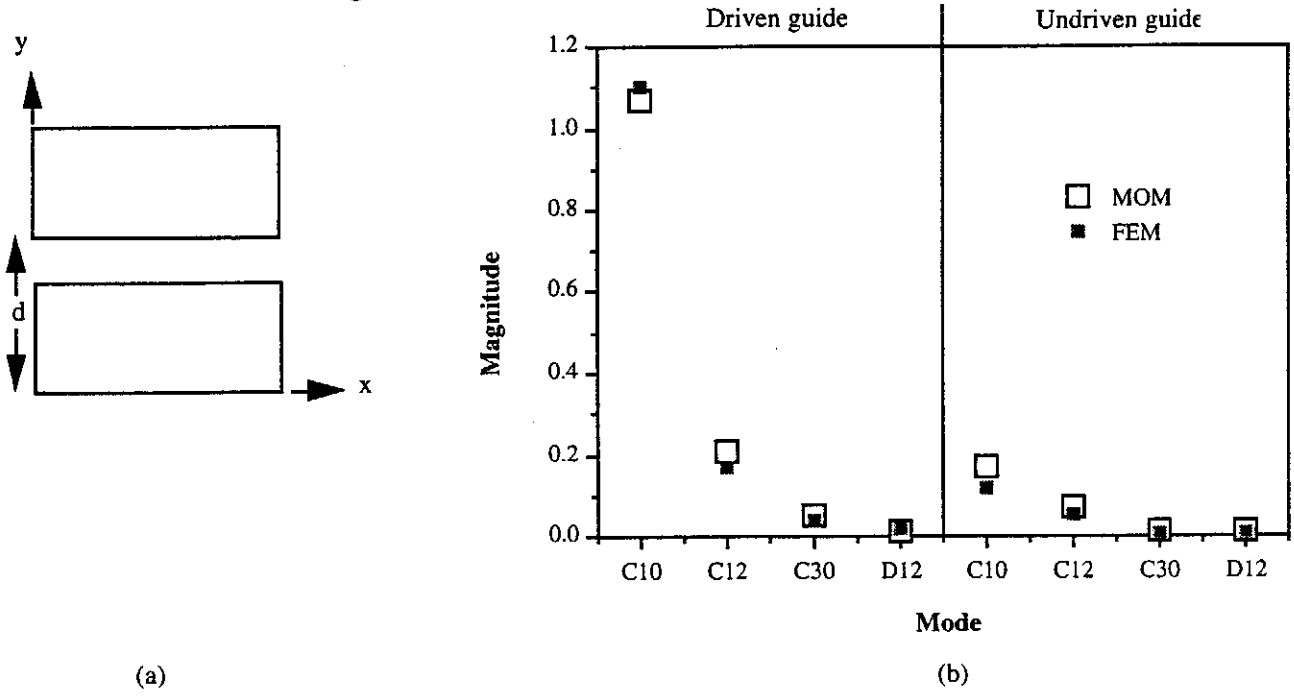

Figure 8 (a) Two aperture geometry. (b) Magnitude of the modal amplitudes for the case of a X band waveguides with d=0.6". The data on the left is for the driven guide, and the data on the right is for the undriven guide.